Materials Letters 120 (2014) 143–146

Contents lists available at ScienceDirect

Materials Letters

journal homepage: www.elsevier.com/locate/matlet

Enhanced electromagnetic absorption properties of reduced graphene oxide–polypyrrole with $NiFe_2O_4$ particles prepared with simple hydrothermal method

Panbo Liu, Ying Huang *, Xiang Zhang

Key Laboratory of Space Applied Physics and Chemistry, Ministry of Education, School of Science, Northwestern Polytechnical University, Xi'an 710129, PR China

ARTICLE INFO

Article history:
Received 26 November 2013
Accepted 11 January 2014
Available online 21 January 2014

Keywords:
Carbon materials
Polymers
Nanoparticles
Dielectrics
Electromagnetic absorption properties

ABSTRACT

The ternary composites of reduced graphene oxide–polypyrrole–$NiFe_2O_4$ (RGO–PPy–$NiFe_2O_4$) were synthesized via a two-step method and the electromagnetic absorption properties were investigated. The average diameter of $NiFe_2O_4$ particles on RGO–PPy ranged from 10 to 20 nm. The results revealed that the electromagnetic absorption properties and the absorption bandwidth of RGO–PPy–$NiFe_2O_4$ are much better than RGO–PPy. The maximum reflection loss of RGO–PPy–$NiFe_2O_4$ is −44.7 dB at 14.9 GHz and the absorption bandwidth with the reflection loss below −10 dB is 4.7 GHz with a thickness of 1.75 mm. Furthermore, our strategy provides a feasible method to obtain the ternary composites with excellent electromagnetic absorption properties and wide absorption bandwidth for future investigators.

1. Introduction

Reduced graphene oxide (RGO) has attracted much attention due to its fascinating properties [1,2]. High dielectric loss and low density enable it to be used as electromagnetic wave absorbers. However, the maximum reflection loss is only −6.9 dB [3]. Based on the impedance matching strategy, one of the effective ways to reduce the problem is to couple RGO with Fe_3O_4 [4,5], Co_3O_4 [6] and $NiFe_2O_4$ nanoparticles [7]. Recently, the ternary composites of EG/PANI/CF [8] and PANI/graphene/Fe_3O_4 [9] have been synthesized, but they exhibit weak absorption properties. Polypyrrole (PPy) is one of the most promising conducting polymers with excellent chemical and physical properties. PPy with magnetic nanoparticles also can be used as electromagnetic wave absorbers [10]. In our recent study, we have studied the electromagnetic absorption properties of RGO–PPy–Co_3O_4, but the synthesis procedure requires multiple steps [11]. Until now, to the best of our knowledge, the electromagnetic absorption properties of the ternary composites consisting of RGO, PPy and $NiFe_2O_4$ particles have never been reported.

In this paper, we have synthesized RGO–PPy–$NiFe_2O_4$ via a two-step method. Structural and morphological properties of RGO–PPy–$NiFe_2O_4$ also have been investigated. The maximum reflection loss of the ternary composites is −44.7 dB and the bandwidth exceeding −10 dB is 4.7 GHz.

2. Experimental

Graphene oxide (GO) was synthesized by Hummers method [12]. Firstly, pyrrole monomer (0.2 mL) with H_2SO_4 (2 mL) and $(NH_4)_2S_2O_8$ (APS, 0.95 g) dissolved in GO solution (100 mL) by sonication treatment, then the solution was cooled down to 0 °C and stirred for 12 h. The precipitate was washed with distilled water. Secondly, $Ni(NO_3)_2 \cdot 6H_2O$ (0.3 g) and $Fe(NO_3)_3 \cdot 9H_2O$ (0.8 g) were added into the solution and stirred, then NH_3H_2O was used to adjust the pH value. The mixture was transferred to a Teflon-lined autoclave and maintained at 180 °C for 12 h. The obtained product was washed with water and dried.

The crystal structure was characterized on X-ray diffraction (D/max 2550 V, Cu Kα radiation). The chemical states were investigated by X-ray photoelectron spectroscopy (XPS, PHI 5300X). The morphology was characterized by field emission transmission electron microscope (FETEM: Tecnai F30G^2). The electromagnetic parameters were measured in a HP8753D vector network analyzer.

3. Results and discussion

The formation mechanism of RGO–PPy–$NiFe_2O_4$ is depicted in Fig. 1a. Firstly, pyrrole monomer absorbs on the surfaces of GO by electrostatic attraction, then initiates to polymerize after adding concentrated H_2SO_4 and APS. Secondly, the reduction of GO and the crystallization of $NiFe_2O_4$ happen in one step by the hydrothermal method. In our experiments, NH_3H_2O is selected

* Corresponding author. Tel.: +86 29 88431636.
E-mail address: yingh@nwpu.edu.cn (Y. Huang).

0167-577X/$ - see front matter © 2014 Elsevier B.V. All rights reserved.
http://dx.doi.org/10.1016/j.matlet.2014.01.054

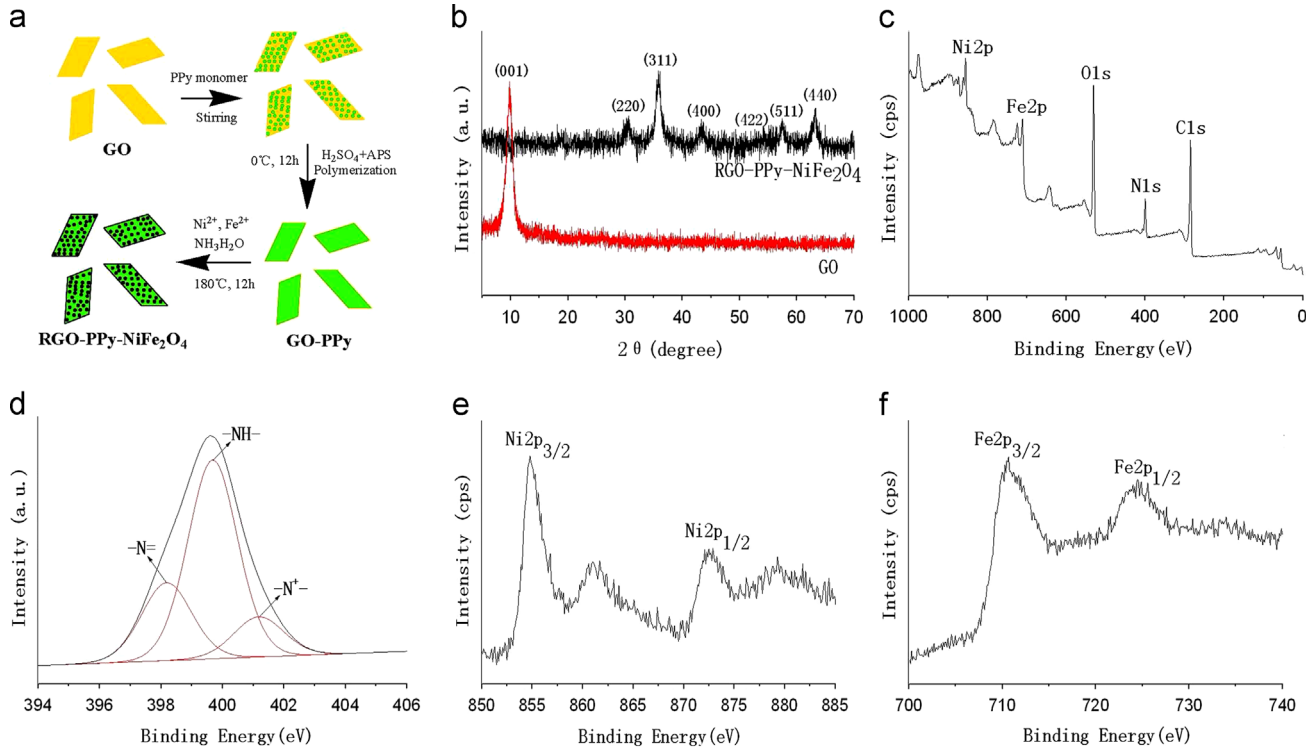

Fig. 1. Schematic illustration (a), XRD patterns of GO and RGO–PPy–$NiFe_2O_4$ (b), XPS spectrum (c), N 1s (d), Ni 2p (e) and Fe 2p (f) spectra of RGO–PPy–$NiFe_2O_4$.

to accomplish the two functions: (1) NH_3H_2O plays an important role in the formation of $NiFe_2O_4$ particles; (2) NH_3H_2O is a reducing agent for the reduction reaction of GO. XRD patterns of GO and RGO–PPy–$NiFe_2O_4$ are shown in Fig. 1b. For GO, the strong peak at 9.8° corresponding to the interlayer spacing of 0.90 nm, which is due to the formation of the oxygen functionalities groups between the layers of GO. For RGO–PPy–$NiFe_2O_4$, the disappearance of the peak at 9.8° indicates the reduction of GO. Furthermore, six diffraction peaks can be assigned to the (220), (311), (400), (422), (511) and (440) planes of $NiFe_2O_4$ (JCPDS card no. 10-0325), suggesting the formation of $NiFe_2O_4$ particles. The relatively weak intensities demonstrate that $NiFe_2O_4$ particles are small. XPS spectra (Fig. 1c) indicate the presence of C, N, O, Fe and Ni elements in RGO–PPy–$NiFe_2O_4$. In Fig. 1d, N 1s XPS spectra can be deconvoluted into three peaks. The peaks at 398.2, 399.7 and 401.3 eV are attributed to the quinoid imine (=N–), the benzenoid amine (–NH–) and the cationic nitrogen atoms ($–N^+–$), respectively. The presence of these peaks suggests the formation of PPy [13]. In Fig. 1e, Ni 2p spectra exhibit two peaks at 854.7 and 872.6 eV, which are assigned to the binding energy of Ni $2p_{3/2}$ and Ni $2p_{1/2}$, respectively. As shown in Fig. 1f, the peaks of Fe $2p_{3/2}$ and Fe $2p_{1/2}$ are located at 710.6 and 724.5 eV, respectively. These results indicate the assembly of $NiFe_2O_4$ particles onto RGO–PPy.

The morphology of the samples is shown in Fig. 2. Fig. 2a shows that RGO sheets are transparent and appear as silky waves, except for some wrinkles at the edges. In Fig. 2b, after decoration with PPy, the surface of RGO becomes rough and some wrinkles uniformly cover on RGO. The SAED pattern (inset in Fig. 2b) indicates that RGO–PPy has no obvious crystalline character, which is due to the perfect coverage of PPy. From Fig. 2c, we can see that large-scale $NiFe_2O_4$ particles with a relatively uniform size distribute on the surface of RGO–PPy, as indicated by the red arrows. In Fig. 2d, it can be observed that the average diameter of $NiFe_2O_4$ particles is in the range of 10–20 nm. The SAED patterns (inset in Fig. 2d) obtained from this region clearly demonstrate the crystalline feature of $NiFe_2O_4$ particles. In order to verify the crystalline structure of $NiFe_2O_4$ particles, we present the HRTEM image of RGO–PPy–$NiFe_2O_4$ in Fig. 2e. All $NiFe_2O_4$ particles show a well-defined lattice plane with perfect crystallinity, and the crystal lattice fringe with a spacing of 0.25 nm (inset in Fig. 2e) can be assigned to the (311) plane of $NiFe_2O_4$ particles. Fig. 2f shows the EDS analysis of RGO–PPy–$NiFe_2O_4$. The results show the presence of C, N, O, Ni and Fe elements in the composites, which is consistent with the results of XPS. Furthermore, the atomic ratio of Ni and Fe (inset in Fig. 2f) is approximately 1:2, the result is consistent with the stoichiometry of $NiFe_2O_4$, indicating the particles are $NiFe_2O_4$.

Fig. 3a shows the real part (ε') and imaginary part (ε'') of the relative complex permittivity of the ternary composites. It can be found that the values of ε' and ε'' are in the range of 6.4–16.4 and 2.2–11.3 respectively. Both ε' and ε'' values decrease gradually with several fluctuations. Fig. 3b shows the real part (μ') and imaginary part (μ'') of the relative complex permeability. It reveals that the values of μ' are in the range of 0.9–1.1 and the μ'' values are less than 0.4 over 2–18 GHz. From Fig. 3c, it can be found that tan δ_μ are largely lower than those of tan δ_ε, indicating that the electromagnetic attenuation mechanism of the ternary composites is mainly dependent on dielectric loss. Furthermore, it demonstrates that RGO–PPy–$NiFe_2O_4$ have better complementarities between dielectric loss and magnetic loss at 13.5–15.1 GHz, which suggests that they have excellent electromagnetic wave absorption properties at this region.

To compare the electromagnetic absorption properties of RGO–PPy and RGO–PPy–$NiFe_2O_4$, the reflection loss (R_L) is calculated by the following equations:

$$R_L(dB) = 20 \log \left| \frac{Z_{in} - 1}{Z_{in} + 1} \right| \quad (1)$$

$$Z_{in} = \sqrt{\mu_r / \varepsilon_r} \tanh\left[j(2\pi f d / c) \sqrt{\varepsilon_r \mu_r} \right] \quad (2)$$